Limiting high-pressure rate coefficient for the recombination reaction FSO3+FSO3FS(O2)O(O2)SF: An experimental and theoretical study

ARTICLE *in* CHEMICAL PHYSICS LETTERS · MARCH 2005

Impact Factor: 1.9 · DOI: 10.1016/j.cplett.2005.01.083

3 AUTHORS:

Adela E. Croce
National University of La Plata
65 PUBLICATIONS **470** CITATIONS
SEE PROFILE

María Eugenia Tucceri
National Scientific and Technical Research …
27 PUBLICATIONS **220** CITATIONS
SEE PROFILE

Carlos J. Cobos
National Scientific and Technical Research …
126 PUBLICATIONS **3,032** CITATIONS
SEE PROFILE

Available online at www.sciencedirect.com
SCIENCE DIRECT®
Chemical Physics Letters 404 (2005) 232–236
CHEMICAL PHYSICS LETTERS
www.elsevier.com/locate/cplett

Limiting high-pressure rate coefficient for the recombination reaction $FSO_2 + FSO_3 \rightarrow FS(O_2)O(O_2)SF$: An experimental and theoretical study

M.E. Tucceri, A.E. Croce, C.J. Cobos *

Instituto de Investigaciones Fisicoquímicas Teóricas y Aplicadas (INIFTA), Departamento de Química, Facultad de Ciencias Exactas, Universidad Nacional de La Plata, CONICET, CICPBA, Casilla de Correo 16, Sucursal 4, (1900) La Plata, Argentina

Received 24 January 2005

Abstract

The kinetics of the recombination reaction $FSO_2 + FSO_3 \rightarrow FS(O_2)O(O_2)SF$ has been studied at 298 K. Both radicals were generated by 193-nm laser flash photolysis of $FS(O_2)O(O_2)SF$ at total CO pressures ranging from 130 to 800 mbar. The decay of FSO_3 radical was monitored by absorption spectroscopy at 450 nm. In all conditions, the reaction was found to be very close to the second-order regime being the limiting high-pressure rate coefficient $(6.5 \pm 1.1) \times 10^{-11}$ cm^3 molecule^{-1} s^{-1}. This value agrees very well with 7.7×10^{-11} cm^3 molecule^{-1} s^{-1}, as derived from statistical adiabatic channel model/classical trajectory calculations on an electronic potential obtained from density functional theory calculations.

1. Introduction

The knowledge of the kinetics of free radical reactions is of major practical importance. In addition to the kinetic information itself, the study of these processes supplies information to the examination and improvement of reaction rate theories. In this context, dissociation–recombination reactions which involve the breaking and making of a simple bond provide a specially searching test for unimolecular reaction theories. In particular, kinetic studies of FSO_3 radical reactions have received a great deal of attention in our laboratory. Early steady-state mechanistic studies [1–5] were more recently followed by real-time resolved experiments [6–11]. In contrast, little is known about the related radical FSO_2. Although no rate coefficients have been reported for the recombination reaction (1)

$$FSO_2 + FSO_3 + M \rightarrow FS(O_2)O(O_2)SF + M \quad (1)$$

this process has been postulated to explain the $FS(O_2)O(O_2)SF$ formation in the stationary photolysis of $FS(O_2)OF$ in the presence of SO_2 and SO_3 [2], and in the mechanism of the thermal reaction of $FS(O_2)$-$OO(O_2)SF$ with CO [3] and of $FS(O_2)OF$ with CO [5]. The FSO_2 is formed in the thermal decomposition of F_2SO_2 under shock tube conditions at 1900–2300 K [12]. A limiting high-pressure rate coefficient for the formation of $^{18}FSO_2$ by association of moderated ^{18}F atoms (generated by neutron irradiation of SF_6) with SO_2 has been measured by a competitive technique [13]. The FSO_2 has been also involved in the mechanism of the plasma chemistry of SF_6/O_2 mixtures [14]. Moreover, FSO_2 radical has been detected and characterized by EPR [15] and ESR [16] spectroscopies. More recently, molecular orbital ab initio calculations of this radical have been reported [17–20]. The FSO_2 formation in SO_2 contaminated areas through the reactions of SO_2 with CF_3O and FO_2 radicals, and their participation in

* Corresponding author. Fax: +54 221 425 4642.
E-mail address: cobos@inifta.unlp.edu.ar (C.J. Cobos).

0009-2614/$ - see front matter © 2005 Elsevier B.V. All rights reserved.
doi:10.1016/j.cplett.2005.01.083

possible ozone depleting catalytic cycles have been suggested [17].

This Letter is concerned with an experimental and theoretical study of reaction (1). The laser flash photolysis technique was used to determine the limiting high-pressure rate coefficient $k_{1,\infty}$ at 298 K. The kinetics was theoretically interpreted in terms of the statistical adiabatic channel model/classical trajectory (SACM/CT) treatment [21,22] on a density functional theory (DFT) potential.

2. Experimental

The setup was basically the same as described previously [6–11,23]. Both FSO_2 and FSO_3 radicals were formed by photodissociation of $FS(O_2)O(O_2)SF$, using the 193 nm line of an ArF excimer laser (Lambda Physik EMG 101 MSC). The progress of reaction (1) was followed by monitoring the FSO_3 by time resolved absorption spectroscopy at 450 nm (spectral resolution, $\Delta\lambda = 1.5$ nm) using a xenon high-pressure arc lamp (Hanovia, 150 W). A crossed-beam geometry between the photolytic and the spectroscopic light beams was used in the present static experiments. After passing through a reaction quartz cell of absorption path length $l = 2.5$ cm, the probe light beam was directed onto the entrance slit of a prism double monochromator (Zeiss MM12) equipped with a photomultiplier tube (RCA, 1P28). The signals were recorded with a digital storage oscilloscope (LeCroy 9400) and further processed with a computer. A digital delay generator (Stanford Research Systems DG535) was interfaced with the laser controlling system and the data acquisition system. Typical laser fluencies of 10–50 mJ cm^2 were measured with a pyroelectric detector (Gentec, DE-500). The laser and analysis beams intensities were recorded with a digital oscilloscope (Nicolet 2090). The gases were handled in a Pyrex vacuum system, and the pressures measured with a pressure transducer (MKS Baratron) and with a quartz spiral gauge.

Due to the high toxicity of $FS(O_2)O(O_2)SF$, this compound was prepared in situ by means of the thermal reaction $FS(O_2)OO(O_2)SF + CO \rightarrow FS(O_2)O(O_2)SF + CO_2$ [3]. Mixtures of 5.7–7.6 mbar of $FS(O_2)OO(O_2)SF$ and 130–800 mbar of CO were introduced in the reaction cell of the photolysis apparatus allowing reacting at least for 30 min at room temperature. Under this conditions the quantitative transformation of $FS(O_2)OO(O_2)SF$ into $FS(O_2)O(O_2)SF$ is achieved [3]. The equilibrated mixtures were then irradiated. $FS(O_2)OO(O_2)SF$ was prepared by photolysis of F_2 in mixtures with SO_3 [24]. CO (Matheson, 99.9%) was passed through traps cooled at 153 K and stored in a Pyrex flask.

3. Results and discussion

3.1. Experimental rate coefficients

The FSO_3 radical exhibits weak diffuse absorption bands at 1300–1400 and 720–840 nm and a discrete band with origin at 516 nm resulting from the C^2E–X^2A_2 transition [25]. The latter is partially overlapped by a fairly strong continuum that decreases in intensity between about 470 and 340 nm [25–27]. At the selected monitoring wavelength of 450 nm, the absorption cross section has been determined to be $\sigma(FSO_3) = (3.64 \pm 0.32) \times 10^{-18}$ cm^2 $molecule^{-1}$ [7]. On the other hand, no experimental data have been reported for the FSO_2 radical. To our knowledge, no $FS(O_2)O(O_2)SF$ photodissociation study has been reported so far. The absence of absorption signals at 300 nm indicates that no FCO radicals ($\sigma(FCO) \approx 1 \times 10^{-18}$ cm^2 $molecule^{-1}$ [28]) are formed. As FCO radicals result from the recombination of CO with the F atoms eventually generated in the photolysis, we conclude that only FSO_2 and FSO_3 radicals are produced in the photolytic primary process. By comparison of the initial FSO_3 absorbance detected immediately after mixing $FS(O_2)OO(O_2)SF$ with CO (photolysis of $FS(O_2)OO(O_2)SF$) and after about 30 min thermal reaction (photolysis of $FS(O_2)O(O_2)SF$), an absorption cross-section for $FS(O_2)O(O_2)SF$ of 3×19^{-19} cm^2 $molecule^{-1}$, roughly estimated on the basis of the experimental value for $FS(O_2)OO(O_2)SF$ of 4.14×10^{-18} cm^2 $molecule^{-1}$ [7], was obtained at 193 nm.

A typical absorbance signal resulting from the photolysis of 7.6 mbar of $FS(O_2)O(O_2)SF$ in the presence of 796.1 mbar of CO is depicted in Fig. 1. This profile is mostly attributed to the removal of FSO_3 by reaction (1). The absence of the F_2SO_2 and SO_3 molecules among

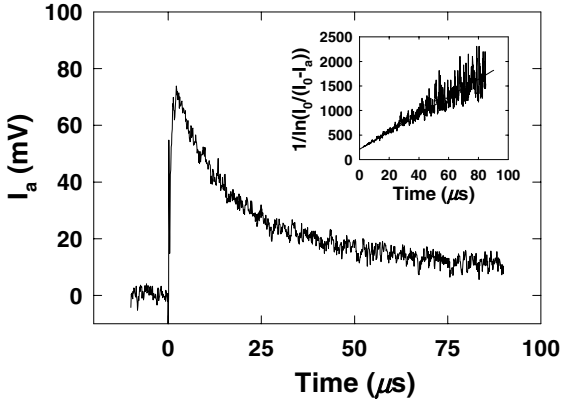

Fig. 1. Time-resolved absorption (I_a) of FSO_3 monitored at 450 nm following the 193-nm photodissociation of 7.6 mbar of $FS(O_2)O(O_2)SF$ in the presence of 796.1 mbar of CO. Insert: $1/\ln(I_0/(I_0 - I_a))$ versus time plot (I_0 is the incident analysis light intensity). The straight line is a fit to the data (see text).

the products of the reaction between $FS(O_2)OO(O_2)SF$ and CO [3] indicates that the reaction $FSO_2 + FSO_3 \rightarrow F_2SO_2 + SO_3$ (which is exothermic in 58.2 kcal mol^{-1} [11,19,29] but probably an activated process) does not occur. On the other hand, due to the fact that reaction $FSO_2 + FSO_3 \rightarrow SO_2 + FS(O_2)OF$ is endothermic in 10.9 kcal mol^{-1} [11,19], we conclude that the only reaction between FSO_2 and FSO_3 radicals is the barrierless recombination (1) (see Section 3.2). From the slope of the second-order kinetic decay plot illustrated in the insert of Fig. 1, a ratio $k_1/\sigma(FSO_3)l = 1.82 \times 10^7$ cm s^{-1} was obtained. Then, the value $k_1 = 6.6 \times 10 -11$ cm^3 $molecule^{-1}$ s^{-1} was derived. In the following we analyze the eventual occurrence of secondary reactions. The microsecond timescale of the experiments indicates that other FSO_3 loss processes are unimportant. In fact, the low values measured for the limiting high-pressure rate coefficients of reactions (2) and (3):

$$FSO_3 + FSO_3 + M \rightarrow FS(O_2)OO(O_2)SF + M \quad (2)$$

$$FSO_3 + CO + M \rightarrow FS(O_2)OCO + M \quad (3)$$

of $(4.5 \pm 0.2) \times 10^{-14}$ cm^3 $molecule^{-1}$ s^{-1} [7,9] and $(4.3 \pm 0.9) \times 10^{-17}$ cm^3 $molecule^{-1}$ s^{-1} [11] (activation energy of 6.8 kcal mol^{-1} [3,5]) preclude their participation in the reaction mechanism. On the other hand, no experimental kinetic data are available for reactions (4a)–(4d)

$$FSO_2 + CO + M \rightarrow FS(O)OCO + M \quad (4a)$$

$$FSO_2 + CO \rightarrow FSO + CO_2 \quad (4b)$$

$$FSO_2 + CO + M \rightarrow F(O_2)SCO + M \quad (4c)$$

$$FSO_2 + CO \rightarrow SO_2 + FCO \quad (4d)$$

The ab initio results detailed in Section 3.2 demonstrate that any of these processes play a role here. Finally, the FSO_2 consumption by the self-reaction processes (5a) and (5b):

$$FSO_2 + FSO_2 + M \rightarrow F(O_2)SS(O_2)F + M \quad (5a)$$

$$FSO_2 + FSO_2 \rightarrow F_2SO_2 + SO_2 \quad (5b)$$

was considered. For this, a numerical simulation of the detected absorption signals with the mechanism formed by reactions (1), (5a) and (5b) was performed. The calculations lead to a fit identical to the depicted in the insert of Fig. 1 when the values $[FSO_3]_{t=0} = 1.2 \times 10^{15}$ cm^3 $molecule^{-1}$, $k_1 = 6.6 \times 10^{-11}$ cm^3 $molecule^{-1}$ s^{-1} and $k_5 = k_{5a} + k_{5b} = 1.5 \times 10^{-13}$ cm^3 $molecule^{-1}$ s^{-1} are used. Further simulations including $\sigma(FSO_2)$ as a free parameter, lead to $[FSO_3]_{t=0} = 1.1 \times 10^{15}$ cm^3 $molecule^{-1}$, $k_1 = 7.3 \times 10^{-11}$ cm^3 $molecule^{-1}$ s^{-1}, $k_5 = 1.6 \times 10^{-13}$ cm^3 $molecule^{-1}$ s^{-1} and $\sigma(FSO_2) = 4.2 \times 19^{-19}$ cm^2 $molecule^{-1}$. Ten recorded signals with CO pressures ranging from about 130 to 800 mbar were analyzed in a similar way. In average, the inclusion of reactions (5a) and (5b) and $\sigma(FSO_2)$ increases k_1 by 8–13% while an upper limit for k_5 of about 2×10^{-13} cm^3 $molecule^{-1}$ s^{-1} was obtained. The small increase in k_1 lies within our stated error limits of about 17% which results from the abovementioned uncertainty in $\sigma(FSO_3)$, and an estimated signal noise of about 10–15%. The obtained $\sigma(FSO_2) \approx 4 \times 19^{-19}$ cm^2 $molecule^{-1}$ is in reasonable agreement with the quantum chemistry predictions discussed in Section 3.2. Nevertheless, in the absence of a realistic experimental value for $\sigma(FSO_2)$, and due to the fact that the uncertainties on the derived k_1 values are small, only the reaction (1) was considered in the present analysis. The derived rate coefficients were found independent of total pressure and were therefore averaged to give the limiting high-pressure rate coefficient,

$$k_{1,\infty} = (6.5 \pm 1.1) \times 10^{-11} \text{ cm}^3 \text{ molecule}^{-1} \text{ s}^{-1}.$$

This value can be compared with those measured for other recombination reactions of the FSO_3 radical in the high pressure region. It is similar to the rate coefficient for the reactions of FSO_3 with F atoms, 7.6×10^{-11} cm^3 $molecule^{-1}$ s^{-1} [6] and Cl atoms, 6.0×10^{-11} cm^3 $molecule^{-1}$ s^{-1} [8]. However, $k_{1,\infty}$ is larger than the rate coefficient measured for the reaction of FSO_3 with FC(O)O radicals of 1.0×10^{-12} cm^3 $molecule^{-1}$ s^{-1} [10,11], and even markedly larger than that determined for the reaction (2) of 4.5×10^{-14} cm^3 $molecule^{-1}$ s^{-1} [7,9].

3.2. Quantum chemical calculations and SACM/CT limiting high-pressure rate coefficients

All quantum chemical calculations were carried out using the Gaussian 98 program package [30]. The energetics of reactions (4a)–(4d) was calculated using the G3(MP2)B3 model chemistry (mean accuracy slightly larger than 1 kcal mol^{-1}) [31]. The large values obtained for the activation energies of reactions (4a) and (4b) of 25.1 kcal mol^{-1} (imaginary frequency $v^{\#} = 147i$ cm^{-1}) and 19.8 kcal mol^{-1} ($v^{\#} = 885i$ cm^{-1}) suggest very low rate coefficients for these processes. The calculations show that reaction (4c) is exothermic in only 0.83 kcal mol^{-1} and, thus, the weakly bound $F(O_2)SCO$ adduct initially formed is not stabilized at all. The abstraction reaction (4d) was found to be endothermic in 4.3 kcal mol^{-1}. This fact and the abovementioned absence of FCO allow us to discard this process. Therefore, the quantum chemical calculations indicate that, under the present experimental conditions, the FSO_2 radical does not react with CO.

To complement the above numerical simulations, the absorption spectrum of FSO_2 is studied using time dependent DFT calculations [32]. To this end, fully optimized geometries were first calculated using the Becke's three-parameters functional [33] with the correlation

functional of Lee, Yang and Parr [34] combined with the large 6-311+G(3df) basis set (B3LYP/6-311+G(3df)). Afterwards, calculations of the relevant electronic transitions of FSO_2 were obtained at the TD-B3LYP/6-311+G(3df) level of theory. In this way an absorption band centered at 413 nm with oscillator strength of 0.010 was found. In a similar way, bands at 472 and 475 nm with oscillator strengths of 0.024 and 0.023 were estimated for FSO_3. These data agree very well with the experimental band located at about 470 nm for which the oscillator strength of 0.05 has been reported [27]. Assuming a Gaussian band profile for FSO_2 similar to the FSO_3 [25,26], we estimate at 450 nm $\sigma(FSO_2) \approx \sigma(FSO_3)/7 \approx 5 \times 10^{-19}$ cm^2 molecule^{-1} in nice agreement with the above modeling calculations.

To perform the SACM/CT calculations for reaction (1) described below, relevant molecular data for the species participant are required. Due to the limited experimental information, they were obtained from B3LYP/6-311+G(3df) calculations. For the sake of simplicity only the relevant input data for the theoretical analysis of $k_{1,\infty}$ are presented. The rotational constants derived from the calculated structural parameters of FSO_2 and FSO_3 are 0.308, 0.298 and 0.162 cm^{-1} and 0.181, 0.171 and 0.171 cm^{-1}. The obtained harmonic vibrational frequencies for $FS(O_2)O(O_2)SF$ are 1510, 1492, 1263, 1247, 837, 836, 780, 714, 619, 543, 540, 508, 471, 439, 411, 313, 290, 272, 140, 80 and 51 cm^{-1}. A $FS(O_2)$–$O(O_2)SF$ bond dissociation energy of $D_e = 75.0$ kcal mol^{-1} was computed at the G3(MP2)B3 level of theory.

The electronic isotropic potential $V(r)$ and the effective rotational constants $B_{eff}(r)$ along the reaction coordinate r (the $FS(O_2)$–$O(O_2)SF$ bond distance) are required to estimate $k_{1,\infty}$. Both were obtained from fully optimized geometries using the UB3LYP/6-311G(d) hybrid functional. Alfa–beta and spatial spin symmetries were destroyed by mixing HOMO and LUMO to obtain accurate unrestricted wavefunctions for singlet states. Fig. 2 shows the computed potential and a fit with the standard Morse function (in kcal mol^{-1}) $V(r) = 77.9\{1 - \exp[-1.47(r - 1.666)]\}^2$ where $r_e = 1.666$ Å. The global agreement between calculated and fitted values is very good. Transformation of the Morse parameter into center-of-mass coordinates gives $\beta \approx 1.53$ Å^{-1}, r_e being close to 2.9 Å. On the other hand, $B_{eff}(r)$ is very well reproduced with the expression (in cm^{-1}) $B_{eff}(r) = [B(r) + C(r)]/2 = 0.0197/[1 + 0.3427(r - 2.9)]$.

The limiting high-pressure rate coefficient for a recombination process is frequently factorized as $k_\infty = f_{rigid} k_\infty^{PST}$ where k_∞^{PST} is the rate coefficient for phase space theory derived with the isotropic part of the potencial and f_{rigid} is the thermal rigidity factor which accounts for anisotropy [35]. The first factor is given by $k_\infty^{PST} = (kT/h)(h^2/2\pi\mu kT)^{3/2} f_e Q_{cent}$. Here μ denotes the collisional reduced mass and $f_e = 0.25$ the electronic

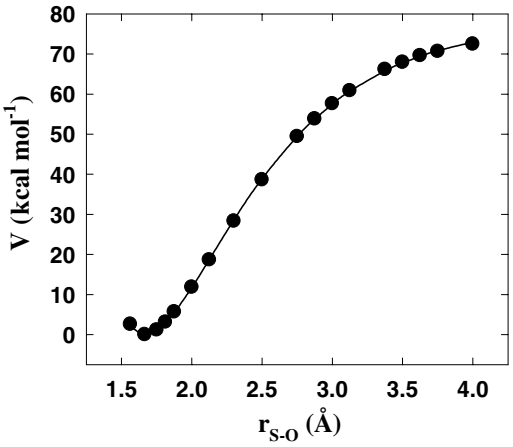

Fig. 2. Potential energy curve for $FS(O_2)O(O_2)SF \rightarrow FSO_2 + FSO_3$. ●: calculations at the UB3LYP/6-311G(d) level; —: fit with a Morse function (see text).

degeneracy factor. The centrifugal partition function is approximated by $Q_{cent} = \Gamma(1 + 1/\nu)(kT/C_\nu)^{1/\nu}$. From the centrifugal barriers obtained with the effective potential $V_{cent}(r) = V(r) + B_{eff}(r)J(J + 1)$ (J is the total angular momentum) we obtain $\nu = 1.08$ and $C_\nu = 2.83 \times 10^{-3}$ cm^{-1}. Then, the values $Q_{cent} = 3.10 \times 10^4$ and $k_\infty^{PST} = 1.64 \times 10^{-10}$ cm^3 molecule^{-1} s^{-1} were calculated at 300 K.

The recent SACM/CT approach which combines the SACM treatment of conserved modes and CT calculations for the transitional modes was employed to calculate f_{rigid} [21,22]. For the low-temperature range $f_{rigid}(T \rightarrow 0)$ is given by $f_{rigid}(T \rightarrow 0) \approx (1 + 0.75Z + Z^4)^{-1/4}$ where $Z = C^n/\gamma$ [T]. For an association of two non identical linear rotors with rotational constants B_1 and B_2 to give a nonlinear adduct with rotors of angle θ between both rotor axes and the molecular axis, C is given by $C = \{2(\varepsilon_s\varepsilon_a\varepsilon_t)^2/[B_1B_2(B_1 + B_2)]\}^{1/3}/2D_e$ and $\gamma = d^{-n}$. For the present reaction, the quanta for the symmetric and asymmetric bending vibrations in the adduct are $\varepsilon_s = 140$ and $\varepsilon_a = 80$ cm^{-1} and the quantum corresponding to the torsional mode is $\varepsilon_t = 51$ cm^{-1}. The B_1 and B_2 values for the FSO_2 and FSO_3 radicals are 0.171 and 0.303 cm^{-1}. The parameter n depends on θ while d depends on θ, ε_s, ε_a and ε_t. An average value for θ of 66° was estimated from the computed $FS(O_2)O(O_2)SF$ structure. As frequently assumed, standard anisotropies were used, i.e. $\alpha/\beta = 0.5$ [21,22,35]. Finally, from calculated values of $C = 0.569$, $d = 2.98$ and $n = 1.28$ results $f_{rigid}(T \rightarrow 0) \approx 0.48$. The transformation of this value to 300 K leads to the SACM/CT estimate of $f_{rigid} \approx 0.47$. The predicted value for k_∞ of 7.71×10^{-11} cm^3 molecule^{-1} s^{-1} compares very well with the experimental of $k_{1,\infty} = (6.5 \pm 1.1) \times 10^{-11}$ cm^3 molecule^{-1} s^{-1}. Over the range 200–400 K we estimate $k_\infty = 7.7 \times 10^{-11} (T/300)^{0.4}$ cm^3 molecule^{-1} s^{-1}.

Acknowledgements

This research project was supported by the Universidad Nacional de La Plata (Project 11/X367), the Consejo Nacional de Investigaciones Científicas y Técnicas (CONICET) (PIP 450), the Comisión de Investigaciones Científicas de la Provincia de Buenos Aires (CICPBA) and the Agencia Nacional de Promoción Científica y Tecnológica (PICT 6786).

References

[1] E. Castellano, H.J. Schumacher, Z. Physik. Chem. NF 44 (1965) 57.
[2] W.H. Basualdo, H.J. Schumacher, Z. Physik. Chem. NF 47 (1965) 57.
[3] R. Gatti, J.E. Sicre, H.J. Schumacher, Z. Physik. Chem. NF 47 (1965) 323.
[4] J. Czarnowski, E. Castellano, H.J. Schumacher, Z. Physik. Chem. NF 57 (1968) 249.
[5] E. Vasini, H.J. Schumacher, Z. Physik. Chem. NF 94 (1975) 39.
[6] A.E. Croce de Cobos, C.J. Cobos, E. Castellano, J. Phys. Chem. 93 (1989) 274.
[7] C.J. Cobos, A.E. Croce de Cobos, H. Hippler, E. Castellano, J. Phys. Chem. 93 (1989) 3089.
[8] A.E. Croce, C.J. Cobos, E. Castellano, Chem. Phys. Lett. 158 (1989) 157.
[9] C.J. Cobos, A.E. Croce, E. Castellano, Int. J. Chem. Kinet. 22 (1990) 289.
[10] M.E. Tucceri, M.P. Badenes, A.E. Croce, C.J. Cobos, Chem. Commun. (2001) 71.
[11] M.E. Tucceri, M.P. Badenes, A.E. Croce, C.J. Cobos, Phys. Chem. Chem. Phys. 3 (2001) 1832.
[12] K.L. Wray, E.V. Feldman, J. Chem. Phys. 54 (1971) 3445.
[13] R. Milstein, R.L. Williams, F.S. Rowland, J. Phys. Chem. 78 (1974) 857.
[14] I.C. Plumb, K.R. Ryan, Plasma Chem. Plasma Process. 9 (1989) 409.
[15] J.R. Morton, K.F. Preston, J. Chem. Phys. 6 (1973) 2657.
[16] Y. Ravi Sekhar, H. Bill, D. Lovy, Chem. Phys. Lett. 136 (1987) 57.
[17] Z. Li, Chem. Phys. Lett. 269 (1997) 128.
[18] Z. Li, J. Phys. Chem. A 101 (1997) 9545.
[19] M.E. Tucceri, M.P. Badenes, C.J. Cobos, Z. Physik. Chem. 214 (2000) 1193.
[20] A.F. Khalizov, P.A. Ariya, Chem. Phys. Lett. 350 (2001) 173.
[21] A.I. Maergoiz, E.E. Nikitin, J. Troe, V.G. Ushakov, J. Chem. Phys. 108 (1998) 9987.
[22] A.I. Maergoiz, E.E. Nikitin, J. Troe, V.G. Ushakov, J. Chem. Phys. 117 (2002) 4201.
[23] M.P. Badenes, A.E. Croce, C.J. Cobos, Phys. Chem. Chem. Phys. 6 (2004) 747.
[24] M. Gambaruto, J.E. Sicre, H.J. Schumacher, J. Fluorine Chem. 5 (1975) 175.
[25] G.W. King, D.P. Santry, C.H. Warren, J. Mol. Spectrosc. 32 (1969) 108.
[26] A.E. Croce, J. Photochem. Photobiol. A: Chem. 51 (1990) 293.
[27] C.J. Cobos, A.E. Croce, E. Castellano, J. Photochem. Photobiol. A: Chem. 84 (1994) 101.
[28] M.M. Maricq, J.J. Szente, G.A. Khitrov, J.S. Francisco, Chem. Phys. Lett. 199 (1992) 71.
[29] M.E. Tucceri, M.P. Badenes, C.J. Cobos, J. Fluorine Chem. 116 (2002) 135.
[30] M.J. Frisch et al., GAUSSIAN 98, Revision A.7, Gaussian, Inc., Pittsburgh, PA, 1998.
[31] A.G. Baboul, L.A. Curtiss, P.C. Redfern, J. Chem. Phys. 110 (1999) 7650.
[32] M.E. Casida, C. Jamorski, K.C. Casida, D.R. Salahub, J. Chem. Phys. 108 (1998) 4439.
[33] A.D. Becke, Phys. Rev. A 38 (1988) 3098.
[34] C. Lee, W. Yang, R.G. Parr, Phys. Rev. B 37 (1988) 785.
[35] C.J. Cobos, J. Troe, J. Chem. Phys. 83 (1985) 1010.